



The following Communications have been judged by at least two referees to be “very important papers” and will be published online at www.angewandte.org soon:

M. Movassaghi,* M. A. Schmidt

Concise Total Synthesis of (–)-Calycanthine, (+)-Chimonanthine, and (+)-Folicanthine

N. Agrawal, Y. A. Hassan, V. M. Ugaz*

A Pocket-Sized Convective PCR Thermocycler

K. Beckerle, R. Manivannan, B. Lian, G.-J. M. Meppelder, G. Raabe, T. P. Spaniol, H. Ebeling, F. Pelascini, R. Mülhaupt, J. Okuda*

Stereospecific Styrene Enchainment at a Titanium Site within a Helical Ligand Framework: Evidence for the Formation of Homochiral Polystyrene

O. Shoji, T. Fujishiro, H. Nakajima, M. Kim, S. Nagano, Y. Shiro, Y. Watanabe*

Hydrogen Peroxide Dependent Monooxygenations by Tricking the Substrate Recognition of Cytochrome P450_{BSF}

M. J. D. Bosdet, W. E. Piers,* T. S. Sorensen, M. Parvez

10a-Aza-10b-borapyrenes: Heterocyclic Analogues of Pyrene with Internalized BN Moieties

M. Lingenfelder,* G. Tomba, G. Costantini, L. C. Ciacchi, A. De Vita, K. Kern

Tracking the Chiral Recognition of Adsorbed Dipeptides at the Single-Molecule Level

Fred Basolo (1920–2007)

Modern Terpyridine Chemistry

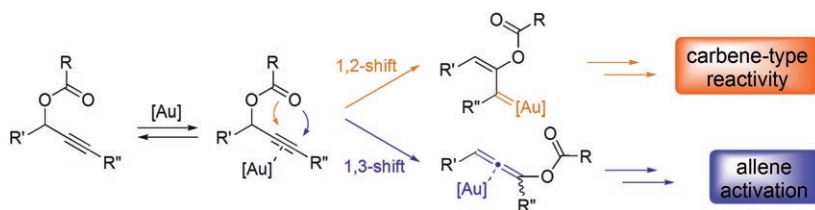
Ulrich S. Schubert, Harald Hofmeier,
George R. Newkome

Obituary

H. Gray, J. S. Magyar ————— 2746

Books

reviewed by E. C. Constable ————— 2748



Shifty business: The use of propargylic esters in Au-based catalysis results in the synthesis of an impressive variety of products as a function of the pendant

groups' functionalities. Skeletal rearrangement by 1,2- and 1,3-migration results in gold–carbene and allene intermediates, respectively.

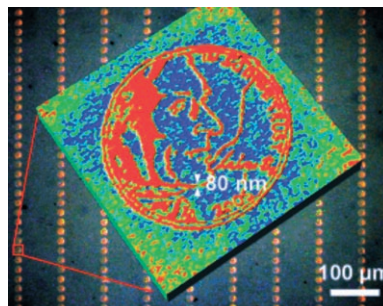
Highlights

Gold Catalysis

N. Marion, S. P. Nolan* — 2750–2752

Propargylic Esters in Gold Catalysis:
Access to Diversity

Neat styles of writing: Recent reports on massively parallel dip-pen nanolithography and further improvements in the resolution of microcontact printing signify that patterning self-assembled monolayers on the submicrometer scale over large areas has now reached a level of sophistication that allows it to rival “hard” lithographic techniques, while retaining the flexibility of using the patterned substrates as a platform for further chemical modification.



Soft Lithography

W. T. S. Huck* ————— 2754–2757

Self-Assembly Meets Nanofabrication:
Recent Developments in Microcontact
Printing and Dip-Pen Nanolithography

Essays

History of Science

M. D. Gordin* ————— 2758–2765

D. I. Mendeleev: Reflecting on His Death in 1907



Periodic law and order: 2007 marks the 100th anniversary of the death of Dmitrii Ivanovich Mendeleev (1834–1907), the Russian chemist best known for formulating the Periodic Table. This Essay looks at Mendeleev in the context of the chemistry and the Russia of his own time and remembers him as the scientist, bureaucrat, and father who died believing that he had begun to put his affairs in order.

Reviews

Palladium Catalysis

E. A. B. Kantchev, C. J. O'Brien,
M. G. Organ* ————— 2768–2813

Palladium Complexes of N-Heterocyclic Carbenes as Catalysts for Cross-Coupling Reactions—A Synthetic Chemist's Perspective

Universal cross-coupling catalysts: Pd⁰ complexes of bulky N-heterocyclic carbene (NHC) ligands show unprecedented substrate scope and high activity. The σ-electron donating NHCs renders the oxidative addition, even into highly functionalized and deactivated substrates, facile whereas the steric bulk expedites reductive elimination. At the same time, the strong Pd–NHC bonds ensure excellent catalyst longevity.



Communications

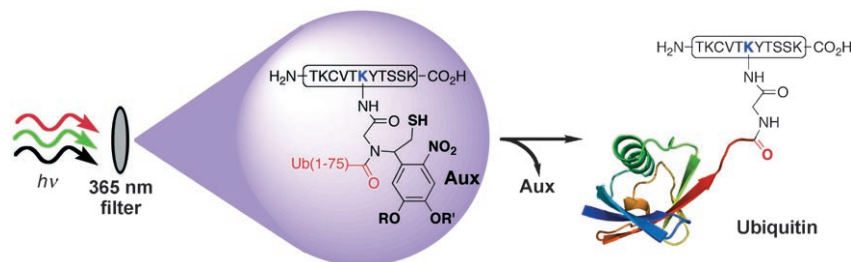


Peptide Ubiquitylation

C. Chatterjee, R. K. McGinty, J.-P. Pellois,
T. W. Muir* ————— 2814–2818



Auxiliary-Mediated Site-Specific Peptide Ubiquitylation



Lighting up ubiquitylation: A photolytically removable ligation auxiliary (Aux) was employed for the site-specific attachment of ubiquitin (Ub) to one of three lysine residues in a C-terminal peptide

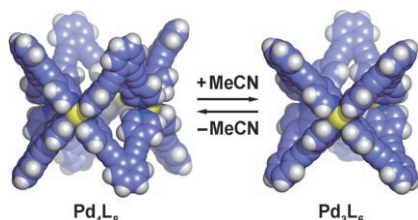
fragment of histone H2B (cH2B). Following photolysis, the ligation was a viable substrate for the ubiquitin C-terminal hydrolase UCH-L3.

For the USA and Canada:

ANGEWANDTE CHEMIE International Edition (ISSN 1433-7851) is published weekly by Wiley-VCH, PO Box 191161, 69451 Weinheim, Germany. Air freight and mailing in the USA by Publications Expediting Inc., 200

Meacham Ave., Elmont, NY 11003. Periodicals postage paid at Jamaica, NY 11431. US POSTMASTER: send address changes to *Angewandte Chemie*, Wiley-VCH, 111 River Street, Hoboken, NJ 07030. Annual subscription price for institutions: US\$ 5685/5168 (valid for print and

electronic / print or electronic delivery); for individuals who are personal members of a national chemical society prices are available on request. Postage and handling charges included. All prices are subject to local VAT/sales tax.

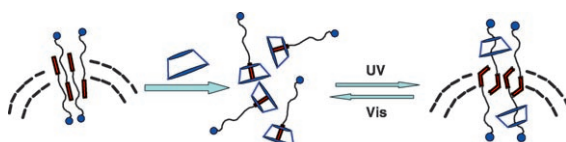


Living in a box: The dynamic self-assembly of Pd_4L_8 and Pd_3L_6 ($\text{L} = 1,2\text{-bis[2-(pyridin-4-yl)ethynyl]benzene}$) box-shaped structures is controlled by the solvent (see picture; Pd yellow, C, N blue, H gray). The two structures can be interconverted reversibly and repeatedly by simply switching the medium between DMSO (Pd_4L_8) and MeCN/DMSO (Pd_3L_6).

Coordination Compounds

K. Suzuki, M. Kawano,
M. Fujita* 2819–2822

Solvato-Controlled Assembly of Pd_3L_6 and Pd_4L_8 Coordination “Boxes”



Inclusion and exclusion of an azobenzene-containing surfactant with α -cyclodextrin (α -CD) can be used to fabricate photostimulus-responsive vesicle-like

aggregates that can undergo assembly and disassembly reversibly (see picture). The movement of α -CD is like that of a molecular shuttle.

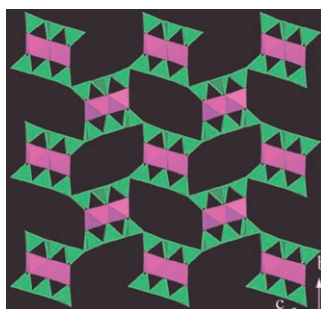
Photoresponsive Vesicles

Y. P. Wang, N. Ma, Z. Q. Wang,
X. Zhang* 2823–2826

Photocontrolled Reversible Supramolecular Assemblies of an Azobenzene-Containing Surfactant with α -Cyclodextrin



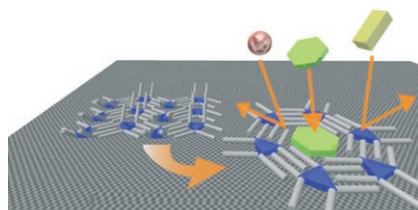
A microporous indate germanate, prepared under mild solvothermal conditions with an organic amine as structure-directing agent, has a structure in which germanate layers (green) are linked by *cis*-edge-sharing chains of In–O octahedra (pink) to form a framework with 1D 12-ring channels (see picture).



Microporous Materials

G.-Z. Liu, S.-T. Zheng,
G.-Y. Yang* 2827–2830

$\text{In}_2\text{Ge}_6\text{O}_{15}(\text{OH})_2(\text{H}_2\text{dien})$: An Open-Framework Indate Germanate with One-Dimensional 12-Ring Channels

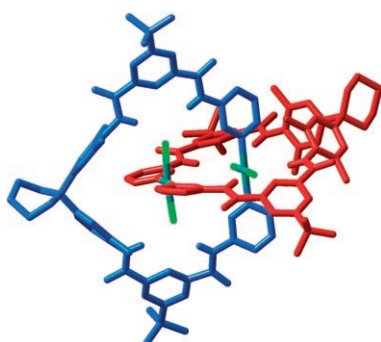


Making honeycomb: The addition of guest molecules to a linear nonporous two-dimensional network results in its transformation into a honeycomb porous network. The transformation shows guest selectivity (see picture).

Host–Guest Chemistry

S. Furukawa, K. Tahara, F. C. De Schryver,
M. Van der Auweraer, Y. Tobe,*
S. De Feyter* 2831–2834

Structural Transformation of a Two-Dimensional Molecular Network in Response to Selective Guest Inclusion



Reversible catenation: A remarkably stable [2]catenane (see picture; Pd turquoise, Cl green) is formed in one step through a combination of first- and second-sphere coordination of a bidentate ligand and the $\{\text{PdCl}_2\}$ metal center. The catenated topology of the two rings can be reversibly converted to the non-interlocked macrocyclic products simply by changing the solvent polarity.

Catenanes

B. A. Blight, J. A. Wisner,*
M. C. Jennings 2835–2838

Reversible Formation of a [2]Catenane through First- and Second-Sphere Coordination



For a Professional Touch

NALIZED • POPULAR • FAST • PERSONALIZED • POPULA

- Reprints of your Article
- High-Resolution PDF
- Personalized Reprints – for example, a bound volume of all your Wiley-VCH articles
– with your company logo and your advertisement



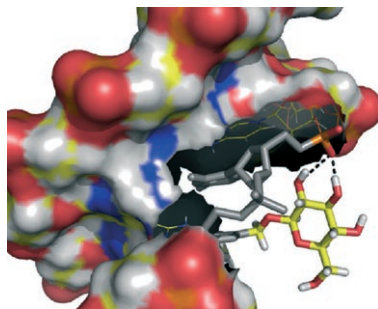
REPRINTS - YOUR TICKET TO SUCCESS! - TO ORDER AT ANY TIME!

 **WILEY-VCH**

 www.wiley-vch.de

Please contact: Carmen Leitner
Chem-reprints@wiley-vch.de

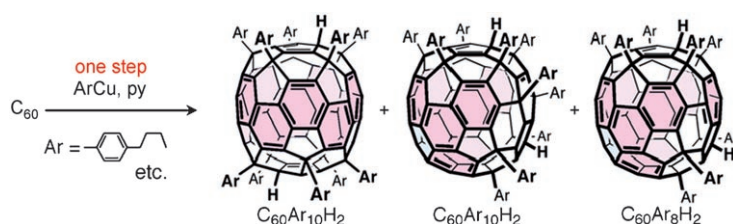
A binding edge? Comparison of dissociation constants and molecular-dynamics snapshots of a panel of synthetic telomeric double-stranded DNA sequences containing HMdU O-glycosides has revealed that the DNA-binding protein of kinetoplastids, such as *Leishmania* and *Trypanosoma*, JBP1, recognizes a critical edge-on conformation of the pyranosyl ring of base J. If this conformation is perturbed, JBP1 binding is dramatically reduced.



Molecular Recognition

R. K. Grover, S. J. K. Pond, Q. Cui, P. Subramaniam, D. A. Case, D. P. Millar, P. Wentworth, Jr.* — 2839–2843

O-Glycoside Orientation Is an Essential Aspect of Base J Recognition by the Kinetoplastid DNA-Binding Protein JBP1



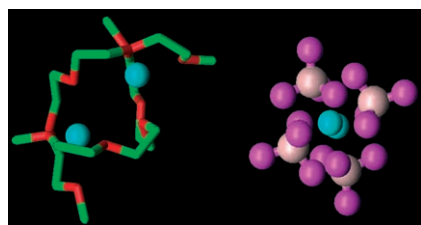
The amount of pyridine (py) is essential for the outcome of the efficient addition of aryl copper compounds to [60]fullerene on a 20-mg to 1-g scale (see scheme). It controls—in addition to the installation of an *ortho*-methyl group on the aryl

reagent—the regioselectivity and the number of aryl groups introduced. The tenfold-addition adduct may be further converted into the corresponding double-decker metallocene.

Functionalization of Fullerene

Y. Matsuo, K. Tahara, K. Morita, K. Matsuo, E. Nakamura* — 2844–2847

Regioselective Eightfold and Tenfold Additions of a Pyridine-Modified Organocopper Reagent to [60]Fullerene

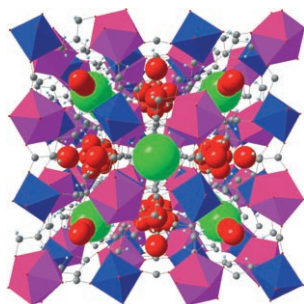


Tunnel route: A new class of solid ionic conductors based on glymes and lithium salts is described. The structure of one example, $(\text{CH}_3\text{O}(\text{CH}_2\text{CH}_2\text{O})_4\text{CH}_3)_{0.5}^- \text{LiBF}_4$, contains two types of tunnels filled by Li^+ ions, which are lined by tetraglyme molecules or BF_4^- ions, respectively (see picture; Li blue, B pink, C green, O red, F purple).

Conducting Materials

C. Zhang, Y. G. Andreev, P. G. Bruce* — 2848–2850

Crystalline Small-Molecule Electrolytes



All aligned: A cubic $3d^5-4f^7$ network of Mn^{2+} and Gd^{3+} ions is assembled by oxydiacetate $(\text{O}(\text{CH}_2\text{CO}_2^-)_2)$. The network, which is reminiscent of Prussian blue analogues (see picture; Gd coordination polyhedra: purple, Mn coordination polyhedra: blue, $[\text{Mn}(\text{H}_2\text{O})_6]^{2+}$: green, H_2O : red), has a weak but definite ferromagnetic interaction.

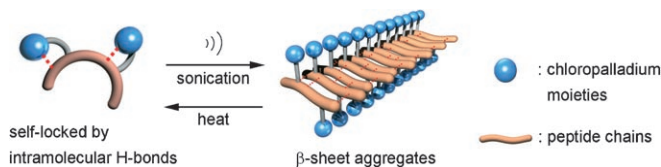
Ferromagnetic Materials

T. K. Prasad, M. V. Rajasekharan,* J.-P. Costes* — 2851–2854

A Cubic $3d-4f$ Structure with Only Ferromagnetic Gd–Mn Interactions

Ultrasound-Induced Gelation

K. Isozaki, H. Takaya,*
T. Naota* — 2855–2857

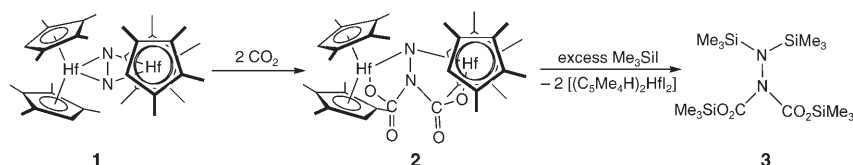


Zap the jello: Stable solutions of a palladium-complexed dipeptide undergo gelation after brief ultrasound irradiation. This is the first case of a reversible, remotely controlled, and rapid sol–gel

transition by H-bonding aggregates. By adjusting the sonication time, the gelation rates and heat-resistant properties of the aggregates can be controlled.

N–C Bond Formation

W. H. Bernskoetter, E. Lobkovsky,
P. J. Chirik* — 2858–2861



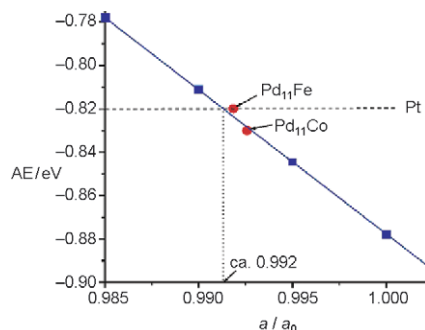
Hafnocene and hydrazine: The addition of two equivalents of carbon dioxide to the hafnocene dinitrogen complex **1** proved effective for the formation of nitrogen–

carbon bonds directly from N_2 and CO_2 . Subsequent treatment of **2** with Me_3SiH liberated the dicarboxylated silyl-substituted hydrazine **3**.

Electrocatalysis

Y. Suo, L. Zhuang,* J. Lu — 2862–2864

First-Principles Considerations in the Design of Pd-Alloy Catalysts for Oxygen Reduction



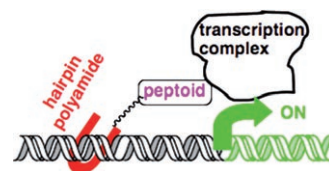
The enhanced catalytic activity of Pd-alloy catalysts in oxygen reduction and the “volcano” relationship between activity and degree of alloying were studied by experiment and DFT calculations. Catalytic activity correlates with adsorption energy (AE) of O_{ads} , which in turn depends on lattice strain (a/a_0) due to alloying. A guideline for the rational design of such catalysts (see picture) predicts that a $Pd_{11}Fe$ alloy will have similar activity to Pt.

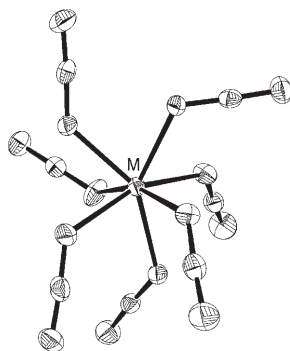
Synthetic Transcription Activator

X. Xiao, P. Yu, H. Lim, D. Sikder,
T. Kodadek* — 2865–2868

A Cell-Permeable Synthetic Transcription Factor Mimic

Do you copy? A cell-permeable synthetic transcription factor mimic composed of a DNA-binding hairpin polyamide and an activation-domain-like peptoid can turn on gene transcription in living cells.





Structures with a bang: The title anions are the first examples of doubly charged heptaazido anions and structurally characterized transition-metal heptaazides. Contrary to the either mon capped octahedral or pentagonal-bipyramidal actinide trianion $[U(N_3)_7]^{3-}$, but in accord with the $[NbF_7]^{2-}$ anion, the title anions have mon capped trigonal-prismatic structures (see picture; $M = Nb, Ta$).

Group 5 Azides

R. Haiges,* J. A. Boatz, M. Yousufuddin, K. O. Christe* — 2869–2874

Mon capped Trigonal-Prismatic Transition-Metal Heptaazides: Syntheses, Properties, and Structures of $[Nb(N_3)_7]^{2-}$ and $[Ta(N_3)_7]^{2-}$



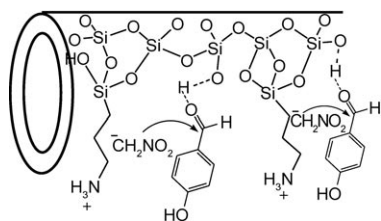
Taking the tube: A silica-supported palladium catalyst packed into teflon tubing is a simple, low-cost, and effective method for carrying out carbonylative cross-coupling reactions of arylhalides with amines and radiolabeled carbon monoxide gas. In carbonylation reactions, the microtube reactor displays enhanced yields over a short time period (12 min) compared with batch methods.



Microfluidic Reactors

P. W. Miller, N. J. Long,* A. J. de Mello, R. Vilar, H. Audrain, D. Bender, J. Passchier, A. Gee — 2875–2878

Rapid Multiphase Carbonylation Reactions by Using a Microtube Reactor: Applications in Positron Emission Tomography ^{11}C -Radiolabeling



Hard graft pays off for Henry: An efficient acid–base bifunctional mesoporous catalyst was prepared by one-step post-synthesis grafting of aminoorganoalkoxysilane groups on mesoporous silica (see picture). The catalyst led to yields of over 99% in the Henry reaction (nitroaldol condensation) of *p*-hydroxybenzaldehyde and nitromethane to form nitrostyrene.

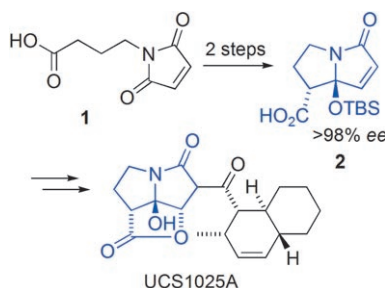
Mesoporous Materials

K. K. Sharma, T. Asefa* — 2879–2882

Efficient Bifunctional Nanocatalysts by Simple Postgrafting of Spatially Isolated Catalytic Groups on Mesoporous Materials



In only two steps the commercially available maleimide **1** is converted into the key pyrrolizidine carboxylic acid unit (**2**) of the telomerase inhibitor UCS1025A. A kinetic resolution through an enantioselective oxa-Michael lactonization and trituration of the resulting scalemic mixture allow for a virtually quantitative separation of a racemate into the enantiomers.



Asymmetric Synthesis

R. M. de Figueiredo, R. Fröhlich, M. Christmann* — 2883–2886

Efficient Synthesis and Resolution of Pyrrolizidines



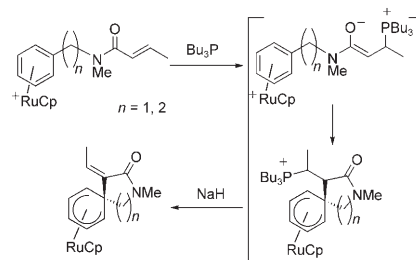
Morita–Baylis–Hillman Reaction

F. C. Pigge,* R. Dhanya,
E. R. Hoefgen _____ 2887–2890



Morita–Baylis–Hillman Cyclizations of
Arene–Ruthenium-Functionalized
Acrylamides

Enticed by metalation with a {CpRu^{III}} fragment, *N*-benzyl and *N*-phenethyl acrylamides participate in phosphine-promoted spirocyclizations even though they are normally unreactive in Morita–Baylis–Hillman (MBH)-type transformations. A ruthenium–arene cation serves as the electrophilic reaction partner for an in situ generated enolate ion in this organometallic variation of the MBH reaction.

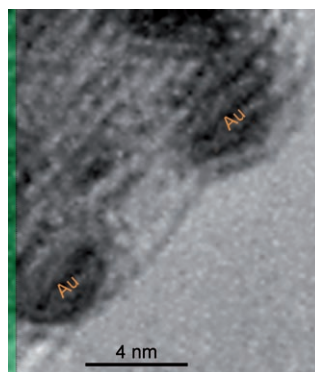


Mesoporous Materials

A. K. Sinha,* K. Suzuki, M. Takahara,
H. Azuma, T. Nonaka,
K. Fukumoto _____ 2891–2894



Mesostructured Manganese Oxide/Gold
Nanoparticle Composites for Extensive
Air Purification



A breath of fresh air: Mesoporous manganese oxide (γ -MnO₂) was deposited with gold nanoparticles by vacuum-UV-assisted laser ablation, resulting in very strong metal–support interactions. The composite was found to remove a wide range of volatile organic compounds (and NO_x and SO₂) from air as well as catalyze their decomposition.

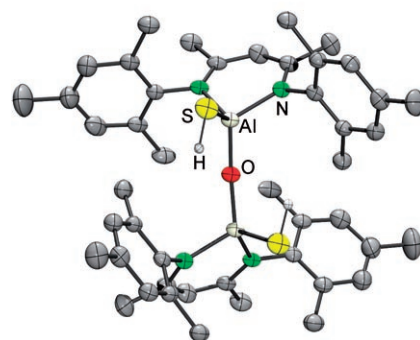
Alumoxanes

S. González-Gallardo, V. Jancik,
R. Cea-Olivares, R. A. Toscano,
M. Moya-Cabrera* _____ 2895–2898



Preparation of Molecular Alumoxane
Hydrides, Hydroxides, and
Hydrogensulfides

Suppressed aggregation: The unprecedented alumoxane hydrogensulfide [{LAl(SH)}₂(μ-O)] and the unique sulfide-bridged compound [{LAl(SH)}₂(μ-S)] can be prepared from the easily accessible aluminum dihydride [LAlH₂] (L = HC-(CMe)₂N(2,4,6-Me₃C₆H₂)₂). Owing to the *cis* conformation of the terminal SH groups, these compounds represent ideal precursors for the synthesis of heterometallic compounds.

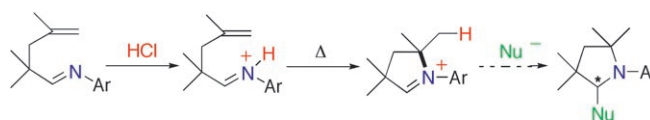


Carbene Precursors

R. Jazzar, R. D. Dewhurst, J.-B. Bourg,
B. Donnadieu, Y. Canac,
G. Bertrand* _____ 2899–2902



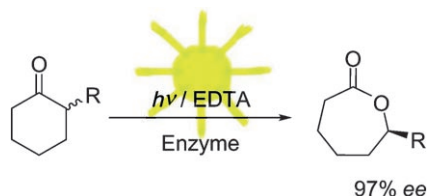
Intramolecular “Hydroiminiumation” of
Alkenes: Application to the Synthesis of
Conjugate Acids of Cyclic Alkyl Amino
Carbenes (CAACs)



A rival for the hydroamination reaction: The intramolecular “hydroiminiumation” reaction features some distinct advantages over intramolecular hydroamination since the resulting prochiral iminium ions

potentially allow the subsequent addition of a large range of nucleophiles to afford a new stereogenic center α to the nitrogen atom (see scheme; Nu[−] = nucleophile).

Let the sunshine in: Light can be used to drive enantioselective Baeyer–Villiger oxidations of cyclic ketones catalyzed by a flavin-dependent enzyme. Photochemical reduction of the flavin using ethylenediaminetetraacetate (EDTA) as the sacrificial electron donor closes the catalytic cycle, thus providing a means to directly regenerate reduced flavin cofactors without the need for costly nicotinamide cofactors as electron donors.



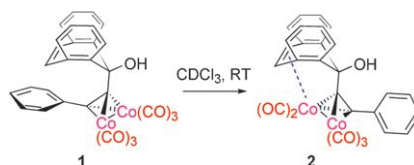
Biocatalysis

F. Hollmann, A. Taglieber, F. Schulz, M. T. Reetz* — 2903 – 2906

A Light-Driven Stereoselective Biocatalytic Oxidation



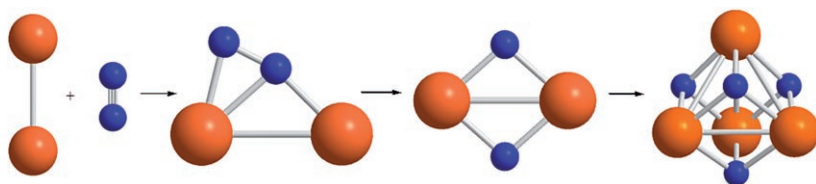
Caught in the act: The [(dibenzosubere-nol) $\text{Co}_2(\text{CO})_6$] cluster **1** (see scheme) loses a carbonyl ligand to yield **2**, the first structurally characterized alkyne–dicobaltpentacarbonyl–alkene complex. This finding provides experimental support for the first step of the proposed mechanism of the Pauson–Khand reaction and yields crucial structural data relevant to computational studies of the process.



Cobalt–Alkyne Complexes

E. V. Banide, H. Müller-Bunz, A. R. Manning, P. Evans,* M. J. McGlinchey* — 2907 – 2910

X-ray Crystal Structure of an Alkyne–Pentacarbonyldicobalt–Alkyne Complex: Isolation of a Stable Magnus-Type Pauson–Khand Reaction Intermediate



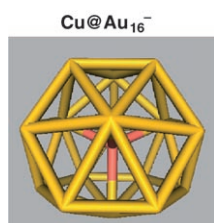
Building up from scratch: The Gd_2 molecule reacts with N_2 in solid argon to form a homoleptic dinuclear dinitrogen complex containing a drastically activated side-on and end-on bonded N_2 ligand (see scheme; Gd orange, N blue). The com-

plex rearranges to a planar cyclic $[\text{Gd}(\mu\text{-N})_2\text{Gd}]$ isomer with a completely cleaved N–N bond, which further dimerizes to form a cubic $[\text{Gd}_4\text{N}_4]$ cluster, a building block for $(\text{GdN})_x$ nanoparticles.

N_2 Activation

M. Zhou,* X. Jin, Y. Gong, J. Li* — 2911 – 2914

Remarkable Dinitrogen Activation and Cleavage by the Gd Dimer: From Dinitrogen Complexes to Ring and Cage Nitrides



Golden cage: The two smallest anionic gold cages, Au_{16}^- and Au_{17}^- , are doped with a Cu atom to give the cluster anions CuAu_{16}^- (see picture) and CuAu_{17}^- , respectively. The photoelectron spectra of CuAu_{16}^- and CuAu_{17}^- suggest that the doping does not alter the structures of the parent cages. Theoretical studies confirm that the Cu atom resides in the center of the gold cages, similar to the situation with endohedral fullerenes.

Gold Cages

L.-M. Wang, S. Bulusu, H.-J. Zhai, X.-C. Zeng,* L.-S. Wang* — 2915 – 2918

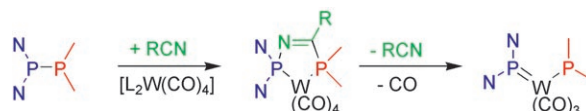
Doping Golden Buckyballs: Cu@Au_{16}^- and Cu@Au_{17}^- Cluster Anions

P–P Insertions

S. Burck, D. Gudat,*
M. Nieger ————— 2919 – 2922



Metal-Assisted, Reversible Phosphinyl Phosphination of the Carbon–Nitrogen Triple Bond in a Nitrile



Split P's: Phosphinyl-substituted N-heterocyclic phosphines react by unprecedented metal-assisted addition of the P–P bond to a nitrile triple bond to give complexes of hybrid bisphosphines. Surprisingly, the addition is reversible, and

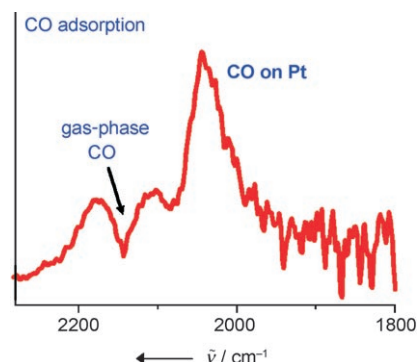
cleavage of the nitrile at high temperature permits controlled access to novel phosphonium–phosphide complexes (see scheme; only crucial parts of the structures are depicted).

Heterogeneous Catalysis

H. Borchert,* D. Fenske, J. Kolny-Olesiak,
J. Parisi, K. Al-Shamery,
M. Bäumer ————— 2923 – 2926



Ligand-Capped Pt Nanocrystals as Oxide-Supported Catalysts: FTIR Spectroscopic Investigations of the Adsorption and Oxidation of CO



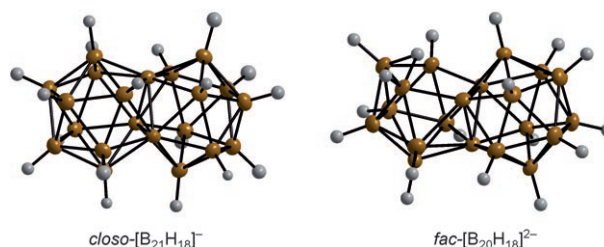
CO oxidation: The suitability of Pt nanoparticles capped with dodecylamine or hexanethiol ligands as oxide-supported catalysts was investigated by FTIR spectroscopy (see picture for the hexanethiol data). It is shown that CO can penetrate the ligand shell and that the Pt nanoparticles possess activity for CO oxidation.

Boron Clusters

E. Bernhardt,* D. J. Brauer, M. Finze,
H. Willner* ————— 2927 – 2930



closo-[B₂₁H₁₈][−]: A Face-Fused Diicosahedral Borate Ion



Siamese borates: Syntheses are described for salts of the *closo*-[B₂₁H₁₈][−] and *fac*-[B₂₀H₁₈]^{2−} ions. The [B₂₁H₁₈][−] ion is the first example of a singly charged *closo*-borate ion in which two icosahedral frag-

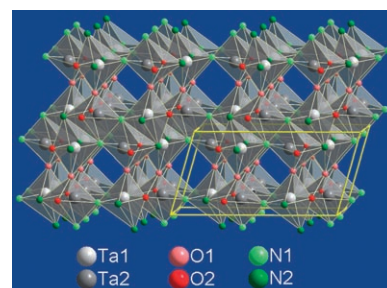
ments are fused together such that they have a common face. The synthesis of novel weakly coordinating anions based on these frameworks is thus within reach.

Tantalum Oxynitride

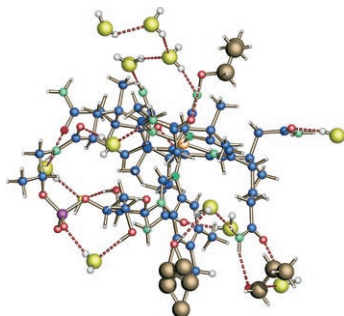
H. Schilling, A. Stork, E. Irran, H. Wolff,
T. Bredow, R. Dronskowski,
M. Lerch* ————— 2931 – 2934

γ-TaON: A Metastable Polymorph of Tantalum Oxynitride

New order: The ammonolysis of β-Ta₂O₅ leads to a new, metastable polymorph of tantalum oxynitride, γ-TaON, which crystallizes in the VO₂(B) structure type (see picture). Quantum-chemical calculations suggest an ordered distribution of the oxygen and nitrogen atoms in the structure and confirm the stability of the new polymorph.



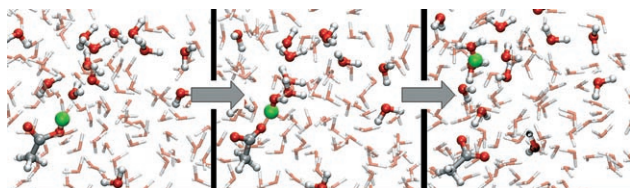
Crystal clear: The experimental charge density of a new solvate of vitamin B₁₂ with more than 250 atoms in the asymmetric unit is determined by high-resolution X-ray diffraction. A data set of approximately 660 000 Bragg reflections is interpreted using a combination of the pseudoatom formalism and quantum-chemical models.



Structural Analysis of Biomolecules

B. Dittrich, T. Koritsanszky, A. Volkov,
S. Mebs, P. Luger* _____ 2935 – 2938

Novel Approaches to the Experimental
Charge Density of Vitamin B₁₂



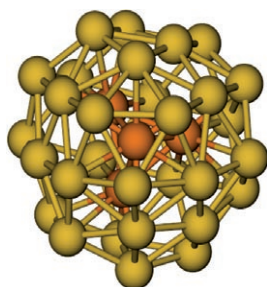
Taking the long way home: The dynamic protonation equilibrium between acetic acid and a water box is studied by molecular dynamics simulations. Two types of motion are found: 1) the proton

is swapped rapidly between acetic acid and a hydrogen-bonded water molecule (see picture); 2) the proton escapes into the bulk volume and rebinds to acetic acid only at a separation of roughly 5 Å.

Proton Transfer

W. Gu, T. Frigato, T. P. Straatsma,
V. Helms* _____ 2939 – 2943

Dynamic Protonation Equilibrium of
Solvated Acetic Acid



Gold prospecting: Trapped-ion electron diffraction, photoelectron spectroscopy, and density functional theory are used to establish the structure of the free gold cluster ion Au₃₄⁻. The results suggest a chiral cluster with an internal trigonal pyramid and C₃ point symmetry.

Gold Clusters

A. Lechtken, D. Schooss,* J. R. Stairs,
M. N. Blom, F. Furche, N. Morgner,
O. Kostko, B. von Issendorff,
M. M. Kappes _____ 2944 – 2948

Au₃₄⁻: A Chiral Gold Cluster?



Supporting information is available on the WWW
(see article for access details).



A video clip is available as Supporting Information
on the WWW (see article for access details).

Angewandte InterScience®
DISCOVER SOMETHING GREAT

“Hot Papers” are chosen by the Editors for their importance in a rapidly evolving field of high current interest. A preview with the graphical abstracts of these articles can be found on the *Angewandte Chemie* homepage in Wiley InterScience at www.angewandte.org.

All articles in *Angewandte Chemie* are published online several weeks ahead of print. They are found under the “EarlyView” link on the journal’s homepage in Wiley InterScience.

Angewandte

Service

Keywords _____ 2950

Authors _____ 2951

Angewandte's Sister Journals _____ 2744

Preview _____ 2953